Parts Per Million CH_4 Chemoresistor Sensors Based on multi wall Carbon Nanotubes/Metal-oxide Nanoparticles

Michela Sainato[1], Md Tanim Humayun[1], Lara Gundel[2], Paul Solomon[3], Liliana Stan[4], Ralu Divan[4], Igor Paprotny[1*]
[1]*University of Illinois at Chicago, Chicago, IL 60607*
[2] *Lawrence Berkeley National Laboratory, Berkeley, CA 94720*
[3]*U. S. Environmental Protection*
[4]*Center for Nanoscale Materials, Argonne National Laboratory, Argonne Il 60439*
paprotny@uic.edu*

Abstract — **This paper presents a novel atomic layer deposition (ALD) based ZnO functionalization of surface pretreated multiwalled carbon nanotubes (MWCNTs) for highly sensitive methane chemoresistive sensors. The temperature optimization of the ALD process leads to enhanced ZnO nanoparticle functionalization and improvement in their crystalline quality as shown by transmission electron microscopy.**
Here we propose a facile and effective top-down method for the high-yield fabrication of chemoresistor sensors making use of MWCNTs/ZnO composite. The behavior of MWCNTs/ZnO sensors in presence of methane concentrations down to 10 ppm level has been investigated. The sensor is currently being tested under a range of conditions that include potentially interfering gases and changes to relative humidity.
Keywords—chemoresistor; carbon nanotubes; metal-oxide nanoparticles; methane.

I. INTRODUCTION

Common hazardous compounds such as NO_x, SO_x, CO, H_2S, NH_3, other nitrogen (e.g. hydrogen cyanide) or sulfur-containing compounds (e.g. organothiols), hydrocarbons (CH_4), volatile organic compounds (benzene, toluene, methanol, etc.) are of major concern for environmental air pollution.
In this context, methane (CH_4) is a potent greenhouse gas with the 100-year global warming potential 28–36 times higher than that of CO_2. [1,2]
The rapidly expanding natural gas infrastructure in the U.S. dictates the need for ubiquitous distributed low-cost, low power, methane sensors with low limit of detection (1 ppm), is critical.

Commercial NO_2 sensors are typically chemi-resistive and make use of semiconducting metal oxides, such as tin oxide (SnO_2), tungsten oxide (WO_3), or zinc oxide (ZnO). Although hey do show excellent sensitivity, limit of detection is typically 100 ppm and operation temperature is in the range of 200–600 °C.[3,4,5] Challenges are reduction of power consumption because of the high operation temperature, as well as improvement of the limit of detection.

Carbon nanotubes (CNTs) are well known for their outstanding tunable electrical properties due to their large aspect ratio (width versus length).[15,16] CNTs are essentially very long aspect ratio cylinders composed of single layers of carbon atoms, allowing most of these atoms to easily interact with surrounding gas molecules. This interaction can potentially translate to strong modulation of electrical conductance of CNTs, resulting in a large relative change in resistance, i.e., high sensitivity. In contrast with other non- CNT based electrochemical and catalytic methane sensors, CNT-based sensors have been shown to detect low concentration of target gases at room temperature, with power consumption of only a few milli-watts.[10-12]

The high sensitivity, low limit of detection, low power requirements, low-cost (due to batch microfabrication process), and low sensitivity to temperature variation[10-12] make CNT-based sensors potentially ideal for out-door methane sensing applications, such as distributed leak detection in natural gas pipelines.
Despite the high potential for modulating electron transport, bare CNTs are insensitive toward most target gases due to poor gas interaction of the pristine graphitic surfaces. Consequently, chemoresistive gas sensing requires either covalent (based on carboxylic acid groups) or noncovalent (based on supramolecular complexation) functionalization of CNTs with analyte-specific entities to enable modulation of their electrical properties in the presence of a target gas.[6]
ZnO nanoparticles have been previously reported as a promising methane sensing materials[18] and promote energetically favorable electron transport at the MWCNTs/ZnO junction compared with previously reported Pd–MWCNT.[10] Consequently, ZnO functionalizing material was suggested for surface pretreated MWCNTs. Three key factors make MWCNTs/ZnO heterostructures one of the most attractive chemoresistive sensors for parts per million level CH_4 detection: (1) strong relative resistance change of ZnO nanoparticles to low concentration level of CH_4; (2) energetically favorable electron transport at MWCNTs/ZnO junction, and; (3) strong electrical current modulation potential

978-1-4799-8287-5/16/$31.00 ©2016 IEEE

due to ballistic transport of electrons through the MWCNTs. This paper focuses on the design and fabrication of a methane sensor based on MWCNTs functionalized with ZnO deposited by ALD.

II. Fabrication of MWCNTs/ZnO Chemoresistor

A. Synthesis of MWCNTs

Synthesis of composite MWCNTs/ZnO nanostructures using ALD deposition is thoroughly investigated. Atomic layer deposition (ALD) allows precise, uniform, and conformal deposition of oxide coatings on geometrically complex substrates, enabling their noncovalent functionalization. [11,17] MWCNTs activated by ZnO nanoparticles deposited on the outer surface by ALD, as given in the literature. [18]

MWCNTs (A batch of 98% pure MWCNT with 12 nm average diameter, 10 μm average lengths, and a specific surface area of ~220 m^2/g was purchased from Sigma Aldrich) were O_2 plasma for 5 min. The ALD method was used to integrate ZnO nanoparticles with surface pretreated MWCNTs. Using diethylzinc (DEZ), $[(C_2H_5)_2Zn]$, as a precursor, the ALD of ZnO (Arradiance Gemstar) on the surface pretreated MWCNTs was performed at various temperatures, from 175 to 220 °C. The deposition process consists of 48 cycles. The ALD process resulted in a deposition of 8 nm ZnO nanoparticles on the MWCNT surface, which was confirmed by transmission electron microscopy (**Fig. 1**).

B. Sensor Fabrication

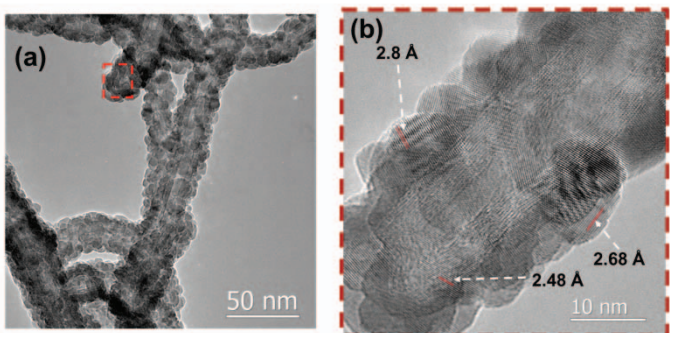

Fig. 1. The transmission electron microscopy (TEM) image show uniform distribution of atomic layer deposited ZnO nanoparticle (NP) layers on the UV-O3 pre-treated MWCNT surface (Fig. 1a). The higher resolution TEM image in Fig. 1b illustrates the wurtzite structure of the ZnO NP and its good crystalline quality. The interplanar spacing of 2.8Å , 2.68Å and 2.48Å correspond to <100>, <002> and <101> planes of ZnO.

On the basis of the results obtained on the preparation of composite MWCNTs/ZnO nanostructures using UV-O3 pre-treatment of MWCNT and ALD for the deposition of ZnO nanoparticles, MWCNTs/ZnO prepared from 10 μm average lengths of MWCNTs pre-treated with 5 min O_2 plasma-treatment coated with ZnO after ALD deposition at 175 °C are selected for the fabrication of chemoresistor devices, because of both the larger specific surface area and enhanced fabrication reliability.

Through a post-process step based on ALD of the CMOS compatible process-flow chemoresistor exploiting a MWCNTs/ZnO as active layer is fabricated.[18] The resulting chemoresistor sensor, namely MWCNTs/ZnO-resistor, specifically consists of a 1 μm thick SiO_2 layer on which the MWCNTs/ZnO layer is integrated between interdigitated electrodes (100 nm Au film on top of a 10 nm Cr and channel lengths of 5 and 10 μm).

III. Sensing

For gas sensing performance evaluation, MWCNTs/ZnO sensors were tested in a sealed test chamber connected with gas inlets and electrical feedthroughs.
A thorough electrical characterization of the MWCNTs/ZnO sensors in CH4 10 ppb at room temperature (RT), using the flow-through technique, is performed. The relative humidity inside the test chamber was kept constant, confirmed by a data-logging humidity sensor (HOBO U-10 series). Synthetic air was used to purge CH_4 from the chamber and to recover the devices to their baseline resistance after each cycle of CH_4 exposure. In order to verify the detection limit at low CH_4 concentration, the change in electrical resistance of the sensors was also monitored. A commercial CH_4 detector (Tpi 721) confirmed the concentration level of CH_4.

IV. Results and Discussion

The ZnO-functionalized MWCNT network exhibits significant resistance change when exposed to CH4 even at a low concentration. The data presented in **Fig. 2** were obtained from MWCNTs/ZnO sensors exposed to a continuous flow of a certified premixed calibration gas containing 10 ppm CH_4 in dry air (supplied by Praxair, Inc.). For all the experiments, flow-rate is maintained at 0.94 liter per minute (L/min), synthetic air is used as carrier gas, relative humidity is set to zero, and temperature is 25 ± 0.5 °C. The sensor is exposed to synthetic air for 45 min prior to run the experiment. This period is necessary to settle the output response of the sensor to a stable current value (warm up period). Afterward the sensors are exposed to NO_2 for 40 min (adsorbing phase) and then to synthetic air for 2h (desorbing phase).

Figure 2 shows the relative resistance $[\Delta R=(R_{methane}-R_{air})/R_{air}]$ of the MWCNTs/ZnO sensors (5 min O_2 plasma-treatment and ZnO ALD at 175°C) increases monotonically while being exposed to 10 ppm of CH_4 at a constant flow rate, and reproducibly returns back to the original levels when purging the test chamber with synthetic air. This result corroborates our hypothesis that the change in resistance is caused by the transfer of electrons from the MWCNT surface to the intermediate complex generated by the ZnO nanoparticles and CH_4 molecules. The relative resistance change for the MWCNTs/ZnO sensors at 10 ppm of CH_4 in dry air was found to be 3.2%.

However, we were only able to test the sensitivity of 175 °C ALD samples, as the adhesiveness of the Au metal pads to external metal wires degrades significantly at higher ALD

Identify applicable sponsor/s here. If no sponsors, delete this text box (*sponsors*).

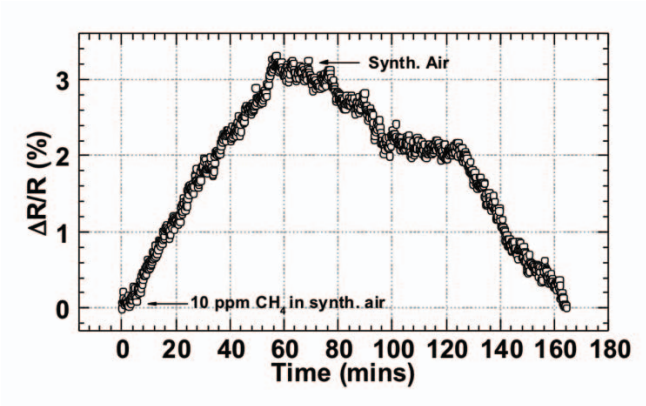

Fig. 2. Relative resistance changes of the 8 nm ZnO functionalized MWCNT (5 min O_2 plasma pretreated) sensor while subjected to repetitive exposure of 10ppm of CH4 in dry air and synthetic air.

temperatures (and superior ZnO crystal quality, the phenomenon).[18] **Fig. 3** illustrates the process flow chart used to fabricate silicon on insulator (SOI)-based shadow mask. The shadow mask based technique offers a resistless alternative electrode fabrication process for the Metal oxides (MOx)-MWCNT chemoresistor sensor. Without affecting the quality of the Au electrodes during the ALD process, this fabrication technique will allow high temperature ALD for the (MOx)-MWCNT with excellent crystal quality of the deposited MOx.

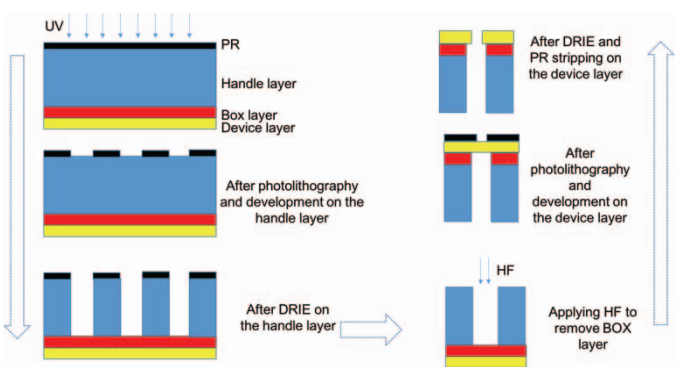

Fig. 3. Silicon on insulator (SOI)-based shadow mask fabrication steps.

ACKNOWLEDGMENT

Use of the Center for Nanoscale Materials, an Office of Science user facility was supported by the U. S. Department of Energy, Office of Science, Office of Basic Energy Sciences, under Contract No. DE-AC02-06CH11357. The project was in part funded by Aclima Inc., award # 2015-07496 and the College of Engineering, University of Illinois, Chicago, IL. Special thanks to D. Rosenmann, Dr. David Gosztola, Dr. Yuzi Liu and Suzanne Miller.

REFERENCES

[1] United States Environmental Protection Agency, "Overview of greenhouse gases," Last accessed August 20, 2015, http://epa.gov/climatechange/ghgemissions/gases/ch4.html.

[2] U.S. Energy Information Administration, "U.S. remained world's largest producer of petroleum and natural gas hydrocarbons in 2014," Last accessed August 30, 2015, http://www.eia.gov/todayinenergy/detail.cfm?id1/420692.

[3] D. Barreca, and D. Bekermann, E. Comini, and A. Devi, R. A. Fischer, A. Gasparotto, C Maccato, G. Sberveglieri, E. Tondello. Sens. Actuators B 2010, 149, 1–7.

[4] P. Fau, M. Sauvan, S. Trautweiler, C. Nayral, L. Erades, A. Maisonnat, B. Chaudret. Sens. Actuators B 2001, 78, 83–88.

[5] T. Waitz, T. Wagner, T. Sauerwald, C.-D. Kohl, M. Tiemann. Adv. Func. Mat. 2009, 19, 653–661.

[6] T. Zhang, S. Mubeen, N. V. Myung, and M. Deshusses, Nanotechnology 19, 332001 (2008).

[7] D. Barreca, D. Bekermann, E. Comini, A. Devi, R. A. Fischer, A. Gasparotto, C. Maccato, G. Sberveglieri, and E. Tondello, Sens. Actuator B 149, 1 (2010).

[8] P. Fau, M. Sauvan, S. Trautweiler, C. Nayral, L. Erades, and A. Maisonnat, Sens. Actuator B. 78, 1 (2001).

[9] T. Waitz, T. Wagner, T. Sauerwald, C. D. Kohl, and M. Tiemann, Adv. Funct. Mater. 19, 653 (2009).

[10] G. Lu, L. Ocola, and J. Chen, Adv. Mater. 21, 2487 (2009).

[11] M. Willinger, G. Neri, E. Rauwel, A. Bonavita, G. Micali, and N. Pinna, Nano Lett. 8, 4201 (2008).

[12] Y. Lu, J. Li, J. Han, H. T. Ng, C. Binder, C. Partridge, and M. Meyyappan, Chem. Phys. Lett. 391, 344 (2004).

[13] C. Massie, G. Stewart, G. McGregor, and J. R. Gilchrist, Sens. Actuator B Chem. 113, 830 (2006).

[14] United States Environmental Protection Agency, "Measurement of the carbon isotopic ratio of atmospheric methane," Last accessed August 20, 2015, http://cfpub.epa.gov/ncer_abstracts/index.cfm/fuseaction/display.abstractDetail/abstract/6351/report/0.

[15] M. S. Dresselhaus, G. Dresselhaus, and R. Saito, Carbon 33 883 (1995).

[16] L. Valentini, I. Armentano, J. M. Kenny, C. Cantalini, L. Lozzi, and S. Santucci, Appl. Phys. Lett. 82, 961 (2003).

[17] S. Boukhalfa, K. Evanoff, and G. Yushin, Energy Environ. Sci. 5, 6872 (2012).

[18] M. Humayun et. al, Journal of Vacuum Science and Technology B 2015, 33(6), 06FF01